Modelling of Thermophysical Properties In EAF-Process And Steelmaking
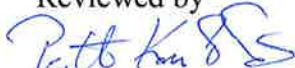
Authors: Karri Penttilä

Confidentiality: Public

Report's title		
Modelling Of Thermophysical Properties In EAF-Process And Steelmaking		
Customer, contact person, address		Order reference
FIMECC_ELEMET2012-13 Research Program		
Project name		Project number/Short name
WP1 - Efficient electric Arc Metallurgy		79759/ FIMECC_ELEMET2012-13/WP1/6
Author(s)		Pages
Karri Penttilä		20
Keywords		Report identification code
EAF, slag foaming, slag viscosity, surface tension, magnetism		VTT-R-00514-14

Summary

The purpose of **EffArc** project was to study different energy efficient methods in the electric arc furnace and steelmaking. A good slag practice is essential for production of a high-quality stainless steel. In addition, the electrical and material efficiency of the electric arc furnace (**EAF**) can considerably be improved by a good slag practice. The metallurgical properties of the slag are strongly influenced by its high-temperature microstructure. Thus, characterization of the phases within the **EAF** slag as well as the determination of the amount of these phases and their compositions is of high importance. This report describes development and validation of advanced computational methods for thermophysical properties of the steel-inclusion system, like density, surface tension and viscosity of the slag phase. Also the effect of magnetic field strength on solidification of steel was studied. **CSFoam**-tool was developed to calculate the foaming index of the slag by using the aforementioned thermophysical properties. The foaming index is a parameter that quantifies the ability of slag to generate foam from either injected gas or gas that is generated within the slag or metal.

Confidentiality	Public

Espoo 27.1.2014

Written by	Reviewed by	Accepted by
Karri Penttilä, Senior Scientist	Pertti Koukkari, Research Professor	Tuulamari Helaja, Technology Manager

VTT's contact address

PO Box 1000, 02044 VTT, Finland

Distribution (customer and VTT)

Contents

1   Introduction

A good slag practice is essential for production of a high-quality stainless steel. In addition, the electrical and material efficiency of the electric arc furnace (**EAF**) can be considerably improved by a good slag practice. The metallurgical properties of the slag are strongly influenced by its high-temperature microstructure. Thus, characterization of the phases within the **EAF** slag as well as the determination of the amount of these phases and their compositions is of high importance.

The **EAF** technology in stainless steelmaking is not completely energy efficient. Main benefits in the **EAF** through the foaming slag practice are [1]:

- Protection of the refractory bricks from the arc.

- Lowering of the electrodes consumption.

- Improving the heat transfer from the arc to the metallic bath.

- Decreasing melting time.

In order to evaluate and quantify the foamability of the slags, the slag's physical properties must be known. In this project novel methods to calculate the viscosity and the surface tension of slags will be implemented. To calculate the density of slags a more simple method is used. Computational thermodynamics will be used as a tool to calculate the amounts and the compositions of the solid phases within the slag in **EAF** process.
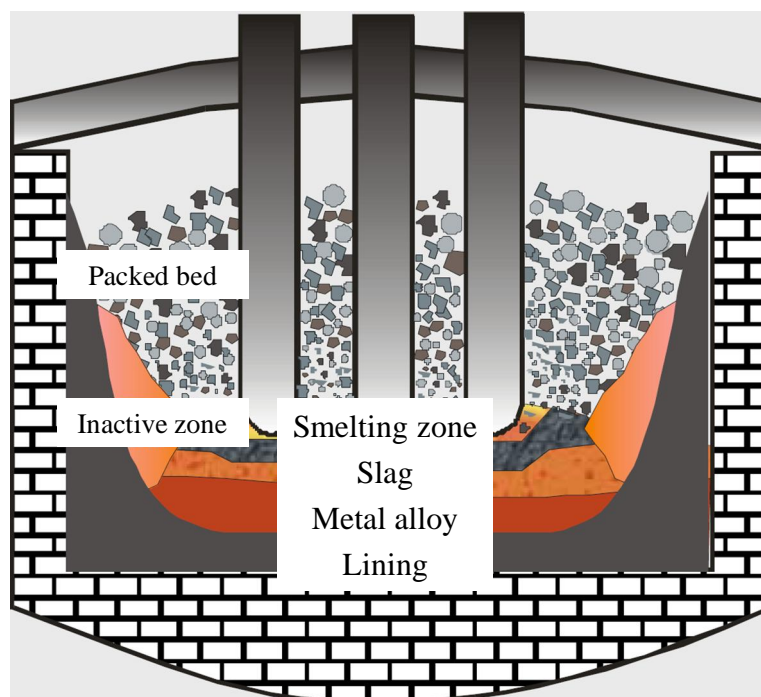

Figure 1. Electric Arc Furnace.

2 Methods

2.1 Factsage

FactSage® was introduced in 2001 as the fusion of the **F*A*C*T** / **FACT-Win** and **ChemSage** thermochemical packages (formerly **SOLGASMIX**). **F*A*C*T** - Facility for the Analysis of Chemical Thermodynamics - started in 1976 as a joint research project between two universities: McGill University (W.T. Thompson) and the École Polytechnique de Montréal (C.W. Bale and A.D. Pelton). The **Windows®** version **FACT-Win** was released in 1999 and offered a fully integrated thermochemical database system that coupled proven software with self-consistent critically assessed thermodynamic data. By this time **F*A*C*T** had expanded well beyond chemical metallurgy and was being employed in other fields of chemical thermodynamics by pyrometallurgists, hydrometallurgists, chemical engineers, corrosion engineers, inorganic chemists, geochemists, ceramists, electrochemists, environmentalists, etc. See Figure 2 for **FactSage** main dialog window.
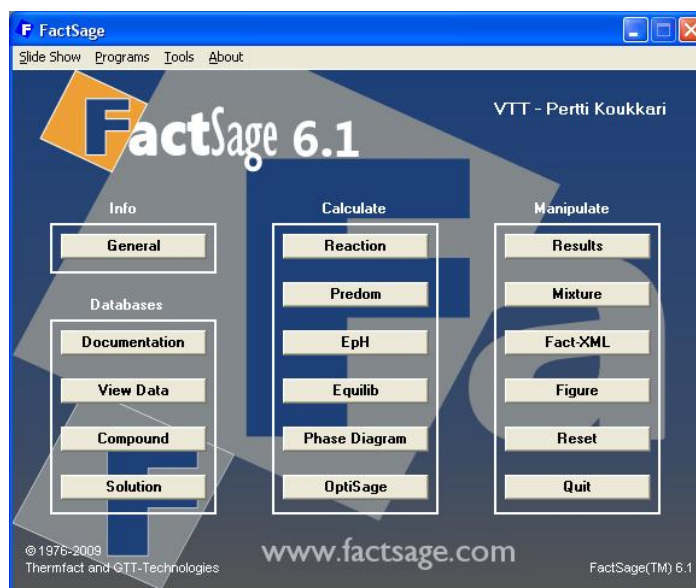
Figure 2. FactSage main dialog window.

In **FactSage** there are two types of thermochemical databases – compound (pure substances) databases and solution databases. The **View Data**, **Compound** and **Solution** modules permit one to list and manipulate the database files.

Compound databases are for stoichiometric solid, liquid and gaseous species such as CaO(s), NaCl(l), SO_2(g). Compound data may include allotropes, for example graphite C(s1) and diamond C(s2), and isomers, for example ethylene C_2H_4O(liq1) and acetylene C_2H_4O (liq2). Depending upon the type of phase (solid, liquid, gas) and data availability, the stored properties include H^o(298.15 K), S^o(298.15 K), C_p(T), magnetic data (Curie or Néel temperature and average magnetic moment per atom), molar volumes (298.15 K) coupled with expansivities, compressibilities and pressure derivatives of bulk moduli as

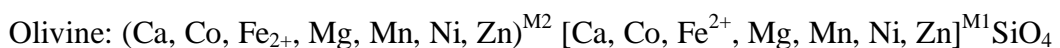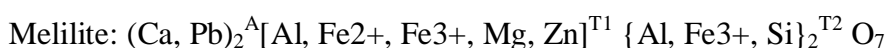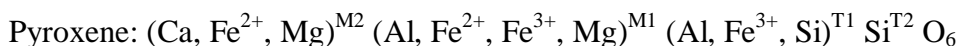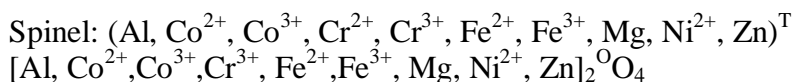functions of T. Infinitely dilute aqueous solution data and non-ideal gas are also stored in the compound databases, as are bibliographical references.

Solution databases are for solid and liquid alloys, carbides, nitrides and carbonitrides, concentrated aqueous solutions, ceramics, salts, mattes, slags, etc. The data are stored in the form of Gibbs energy functions for the phase constituents and temperature dependent model parameters for calculating the Gibbs energy of mixing among the phase constituents. **FactSage** supports more than 10 different solution models including simple polynomial models (Redlich-Kister and Legendre polynomials) combined with different higher order extrapolations (Muggianu, Kohler, Toop), the Unified Interaction Parameter Model, Modified Quasichemical models for short-range ordering in pair and quadruplet approximations, the Pitzer model (for concentrated aqueous solutions) and sublattice models such as the Compound Energy Formalism. Additional solution models are constantly planned.

FToxid Liquid oxide database

FToxid - oxide database for slags, glasses, minerals, ceramics, refractories, etc. contains data for stoichiometric oxides and oxide solutions of the following components: Al_2O_3, As_2O_3, B_2O_3, CaO, CoO, CrO, Cr_2O_3, Cu_2O, FeO, Fe_2O_3, GeO_2, K_2O, MgO, MnO, Na_2O, NiO, PbO, SiO_2, SnO, TiO_2, Ti_2O_3, ZnO, ZrO_2. Not all binary, ternary and higher-order sub-systems have been evaluated and optimized, nor are all composition ranges covered. However, the system Al_2O_3-CaO-FeO-Fe_2O_3-MgO-SiO_2 has been fully optimized from 25 ^{o}C to above the liquidus temperatures at all compositions and oxygen partial pressures. Components CoO, CrO, Cr_2O_3, Cu_2O, MnO, NiO, PbO, SnO, TiO_2, Ti_2O_3, ZnO and ZrO_2 were added to this core six-component system and the relevant subsystems were optimized over the composition ranges important for applications in ferrous and non-ferrous metallurgy, production of ceramics, refractories and paint pigments. Currently there is work to include B_2O_3, K_2O and Na_2O to the core six-component system for applications in the glass industry, combustion, coal gasification and waste management. The liquid/glass solution phase is called FToxid-Slag. As well as all the oxide components mentioned above, it includes dilute solutions of S, SO_4, PO_4, H_2O/OH, CO_3, F, Cl, I.

There are many oxide solid solutions in the database. Some of the most extensive solutions include:

Spinel: $(Al, Co^{2+}, Co^{3+}, Cr^{2+}, Cr^{3+}, Fe^{2+}, Fe^{3+}, Mg, Ni^{2+}, Zn)^T$
$[Al, Co^{2+}, Co^{3+}, Cr^{3+}, Fe^{2+}, Fe^{3+}, Mg, Ni^{2+}, Zn]_2^O O_4$

Pyroxene: $(Ca, Fe^{2+}, Mg)^{M2} (Al, Fe^{2+}, Fe^{3+}, Mg)^{M1} (Al, Fe^{3+}, Si)^{T1} Si^{T2} O_6$

Melilite: $(Ca, Pb)_2^A [Al, Fe2+, Fe3+, Mg, Zn]^{T1} \{Al, Fe3+, Si\}_2^{T2} O_7$

Olivine: $(Ca, Co, Fe_{2+}, Mg, Mn, Ni, Zn)^{M2} [Ca, Co, Fe^{2+}, Mg, Mn, Ni, Zn]^{M1} SiO_4$

FSstel Steel database

FSstel - steel database contains data for 115 completely assessed binary alloy systems, 85 ternary and 17 quaternary systems that include the elements: Al, B,

Bi, C, Ca, Ce, Co, Cr, Cu, Fe, La, Mg, Mn, Mo, N, O, Nb, Ni, P, Pb, S, Sb, Si, Sn, Ti, V, W, Zr. It is intended to provide a sound basis for calculations covering a wide range of steelmaking processes, e.g. reduction of oxygen and sulphur concentration levels through deoxidation and desulphurization of the melt; constitution of a wide range of steels, including austenitic, ferritic and duplex stainless steels and including carbide and nitride formation.

2.2   ChemSheet

Chemsheet works as an add-in program of general thermodynamics in Excel [2] (see Figure 3). The thermochemical programming library **ChemApp** is used in combination with its application-specific thermochemical data. The non-ideal solution models cover concentrated aqueous solutions, dilute and concentrated alloys, liquid slags and molten salts, solid solutions, non-ideal gases and non-stoichiometric systems. **ChemSheet** is straightforward and easy to use and requires no programming skills other than normal Excel use. To the user, the process model can be just one Excel-file.
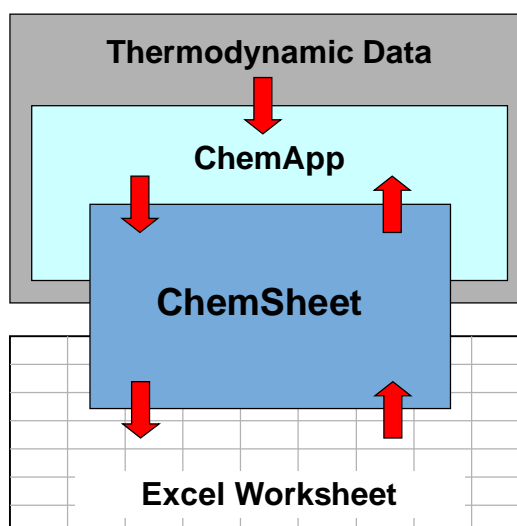

Figure 3 ChemSheet Interface.

In **ChemSheet** as in **ChemApp** there are two different calculation methods: using global conditions of the System, or using Streams. Using Global conditions, user merely needs to set single values for temperature and pressure, and enter incoming constituents to define the initial composition of the system. A stream is a means for transferring non-reacted matter to a reaction zone. It has constant temperature and pressure, and contains one or more constituents. When using Streams, you set the three variables: temperature, pressure and composition for each input stream and set single conditions for temperature and pressure of the system

ChemSheet can calculate one or more equilibrium steps. For each step user needs to define the initial conditions, either global or stream conditions (equilibrium temperature, pressure and the initial composition, and same for any incoming streams, its temperature, pressure and composition). **ChemSheet** contains one variable (worksheet name variable), *StepIndex*, that can be used in formulas so

that values of these conditions can vary between the steps (for example to change the equilibrium temperature between the steps).

In this project **ChemSheet** is used for the thermodynamic calculation of the corium system. The calculated results (like composition of the molten oxide phase) are stored directly to Excel worksheet cells and then it easy to use them as input for the calculation of the viscosity model, as **CSFoam** tool used for it is also implemented as an Excel add-in.

2.3 Thermodynamic system

Thermodynamic system for **ChemSheet** can be generated in **FactSage** and then exported as a thermodynamic file (so called transparent data-file, which is in binary, encrypted formed, if it contains any solution data). Figure 4 shows selection of solution/mixture phases that are found from the **FSstel** database for the given reactants. These reactants include all the components that are needed for the calculation of the electric arc furnace system.
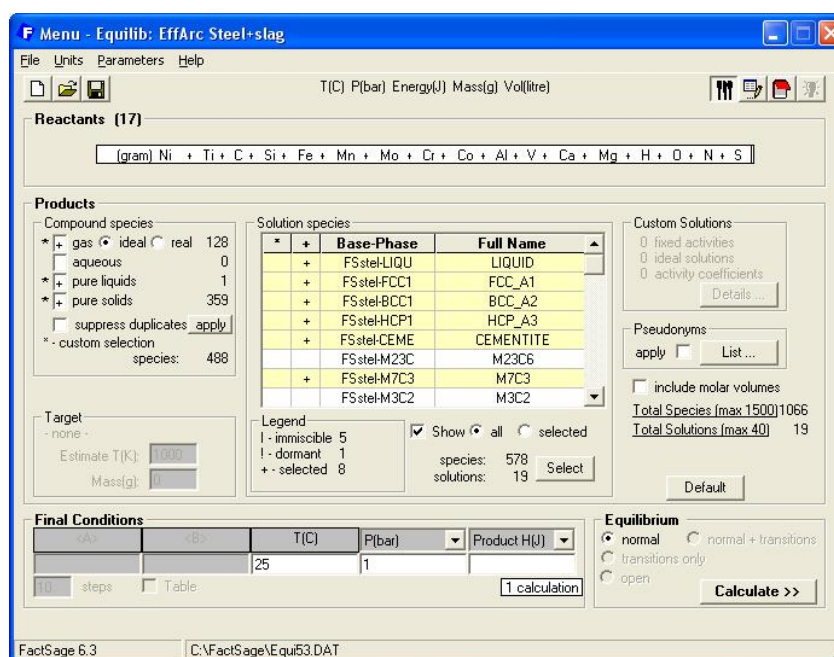

Figure 4. Selected steel + oxide slag system in FactSage.

The included elements are: Al, C, Ca, Co, Cr, Fe, H, Mg, Mn, Mo, N, Ni, O, S, Si, Ti, V. All together there 128 gas phase species, 19 solution phases containing 578 species, one pure liquid phase (water) and 359 pure solid phases (mainly pure metals and oxides). The two most important solution phases are the liquid steel (LIQUID) and the liquid oxide phase (SLAGA). Liquid steel phase contains 28 constituents; metals, oxides and sulphides. It describes the molten steel phase. The constituents in the liquid steel phase are (as named in the FSstel database): Al2O3, SiO2, CaO, FeO, Fe2O3, MgO, CoO, NiO, MnO, CrO, Cr2O3, Ti2O3, TiO2, Mn2O3, Al2S3, SiS2, FeS, Fe2S3, MgS, CoS, NiS, MnS, CrS, Cr2S3, Ti2S3, TiS2, Mn2S3. Liquid oxide phase contains 36 constituents; metals, oxides and sulphides as well. It describes the formed slag phase on the surface of the liquid steel where metals have been oxidized by air. There are two instances of this

phase in the thermodynamic system (SLAGA#1 and SLAGA #2) as it can separate into two immiscible phases. This means that these two phases and their constituents have same the thermodynamic parameters (same reference states and interaction energies) but their phase compositions are different. The constituents in the SLAG phase are (as named in the FSstel database): Fe, C, Co, Cr, Al, Mn, Mo, N, Ni, S, Si, Ti, V, Mg, O, AlO, Al2O, CrO, Cr2O, MnO, SiO, TiO, VO, Ti2O, V2O, MgO, FeS, MnS, Ca, CaO, CrS, NiS, TiS, VS, CaS, MgS.

2.4 Electric arc model

Thermodynamic modelling software ChemSheet was used for calculating the equilibrium composition in the **EAF**. One goal of the calculation is to determine the composition and properties of the slag phase layer when different slag forming components are added. Slag layer is formed on top of the liquid steel. The liquid steel and slag mixture in the furnace is described as a thermodynamic system. The thermo-dynamic data is acquired from the FactSage software databases (shown in Chapter 2.3). The model calculates the global equilibrium between the given raw materials at different temperatures. As a result it returns the composition of the furnace, i.e. the masses and mass fractions of the slag phase(s), the steel phase and any remaining solids (inclusion) phases. It also calculates the foaming index of the slag with **CSFoam**-tool (see Chapter 2.6).

2.5 Foaming

Slag foaming phenomena are observed in many ferrous pyro-metallurgical processes and are of interest in steelmaking. The slag foaming has become important for the modern electric arc furnace (**EAF**). The foaming practices are used to shield the refractory from the arc. The foamed slag stabilizes the arc, shields the metal from the atmosphere and improves the energy efficiency. The control of foaming height is required to maintain a steady operation. Foam acts as a thermal insulator between the hot bath and the surroundings thus reducing the electrical power required to maintain the high operating temperature and limiting electrode consumption. Foaming slag stabilizes the striking of the arc. This leads to a higher power input at a constant voltage. By applying the reproducible slag practice in stainless steel the heat transfer increases between arcs and the metal, heat radiation is screened, chromium losses to slag decreases, electron consumption decrease due to longer arcs, the need of injection material decrease. Foaming also promotes chromium recovery [1].

The foaming index is a parameter that quantifies the ability of slag to generate foam from either injected gas or gas that is generated within the slag or metal. In the case of ideal slagging, the foaming index is equal to the average foam life. The foaming index decreases with increasing viscosity and increases with decreasing viscosity. Various techniques based on dimensional analysis of the kinetic properties of the slag have been applied in order to find the relationship describing the foaming index.

In the industrial experiments the control methods of the slag foaming operations are based on the visual observation or on noise emitted by the **EAF**-furnace. The lower Cr_2O_3 content slags and large initial FeO-content slags are more foaming.

The foaming is also observed to promote chromium recovery. The foaming index for the slags is observed to be relatively similar, due to the similarities between viscosity, density and surface energy values, although their compositions are quite different. The foaming capability of slags can be enhanced by addition of appropriate materials such as limestone and calcium nitrate.

In an ideal system for which the gas voidage ε and the superficial velocity U are uniform, the foaming index Σ could be related to the traveling time of the gas bubbles t in the slag having foam height Δh:

$$\tau = \frac{\Delta h}{U/\varepsilon} = \Sigma \qquad\qquad (1)$$

Generic empirical model derived from dimensional analysis for foaming index can be given as:

$$\Sigma = K \frac{\eta}{\sqrt{\sigma\rho}} \qquad\qquad (2)$$

where K is empirical constant, η is the viscosity, ρ is the density and σ is the surface tension of the slag.

The reactions that generate gas bubbles are of course required the slag foaming and the physical and chemical characteristics of the slag have to sustain the gas bubbles.

2.6 CSFoam

CSFoam tool was developed in this project for the calculation of physical properties of oxide slags in steel making. In the case of electric arc furnace it is used for the calculation of the slag foaming which is dependent on the slag viscosity, surface tension and density.

CSFoam tool is an Excel add-in like **ChemSheet**. It contains internal database for selected components and three functions to calculate the viscosity, the surface tension, and the density. The interfaces of these routines are shown in Table 1.

*Table 1. **CSFoam** routines with input parameters.*

Property	Param1	Param2	Param3	Param4	Param5
VISCOSITY	TEMPERATURE	COMPOSITION	NAMES	COMP_UNIT	PROP_UNIT
TENSION	TEMPERATURE	COMPOSITION	NAMES	COMP_UNIT	PROP_UNIT
DENSITY	TEMPERATURE	COMPOSITION	NAMES	COMP_UNIT	PROP_UNIT

Here is a description of routines and their parameters.

PROPERTY: If property is **TENSION** then it can be used for returning the surface phase composition as well. In order to do this select a range containing as many cells as there are number of compounds plus one. Then enter the parameters as normally and finally press CTRL+SHIFT+ENTER.

TEMPERATURE: Value can be a constant, a formula or a reference to worksheet cell.

COMPOSITION: Value can be a constant array, a formula array or a reference to worksheet range of cells.

NAMES: Value can be a constant array or a reference to worksheet range of cells.

COMP_UNIT: Unit of composition. Value can be a constant or a reference to worksheet cell. Valid units are: *"kg", "mol"*.

PROP_UNIT: Unit of calculated property. Value can be a constant or a reference to worksheet cell. Valid units for **DENSITY** are: *"kg/m3", "kg/dm3", "g/cm3", "m3/mol", "cm3/mol", "mol/m3", "mol/cm3"*; valid units for **TENSION**: *"N/m", "mN/m"*; valid units for **VISCOSITY** are *"Pas"*.

Figure 5 shows an example how a property value (in this case density) can be calculated in Excel worksheet.

Figure 5. Using a function in worksheet to calculate the density of molten oxide

2.7 Viscosity model

Assuming that the structure of aluminosilicate melts consists of only three kinds of chemical bonds, i.e. Si–BO (bridging oxygen in Si tetrahedral unit), Al–BO (bridging oxygen in Al tetrahedral unit with a charge-compensating cation), and Si–NBO (NBO: non-bridging oxygen connected with Si) with a charge-compensating cation (see Figure 6), it is possible to calculate the bonding states of oxygen in molten aluminosilicate by the chemical composition of slag without any thermodynamic parameters. Owing to a simple method, the evaluation of the bonding states of oxygen can be conducted in various kinds of silicate systems including alkali oxides as well as alkaline earth oxides. Silicate slag has a network structure made of bonding SiO_4^{4-} units and Si tetrahedral ions. Si tetrahedral ions are combined through bridging oxygen.

The non-bridging oxygen ion O^- and the free oxygen ion O^{2-} are generated by partially cutting off the network structure of Si tetrahedral when adding some basic oxides such as CaO and Na_2O in silicate slag. The non-bridging oxygen ion and the free oxygen ion have a larger mobility than the bridging oxygen in the network structure because there are "cutting-off" points. It is assumed that the movements of "cutting-off" points cause a viscous flow that lowers the activation energy of viscosity [3].
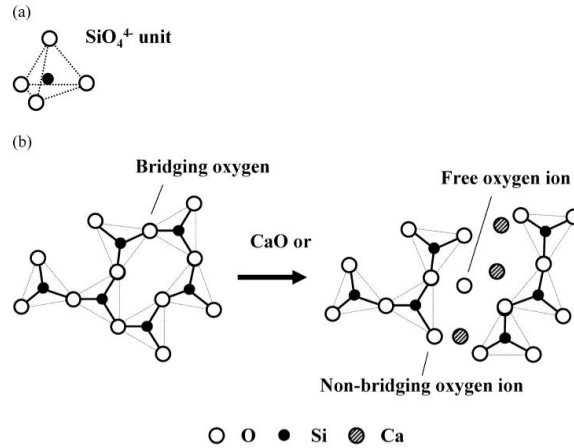
Figure 6. Structure of silicate slag.

Originally this method was applied to system of SiO_2–CaO–MgO–FeO–K_2O–Na_2O–Al_2O_3 system describing aluminosilicate melts containing alkali oxides in melting furnaces. Since then CrO, Cr_2O_3, Fe_2O_3, NiO, TiO_2, have been added.

The viscosity on liquid oxide is calculated as:

$$\eta = A \cdot \exp\left(\frac{E_v}{R \cdot T}\right) \tag{3}$$

where A is a constant (4.80×10^{-8}), E_v is the activation energy, R is the gas constant (8.314), and T is the temperature. The activation energy is calculated as:

$$E_v = \frac{E}{1 + \sqrt{\sum_i \alpha_i \cdot N_{(NBO+FO)_i} + \sum_j \alpha_{j\,in\,Al} \cdot N_{(Al-BO)_j}}} \tag{4}$$

where E is the activation energy of pure SiO_2 (5.21×10^5), α_i and α_j are model parameters in Table 2, $N_{(NBO+FO)}$ of the sum of the fractions of non-bridging oxygen ion (NBO) and free oxygen ion (FO), $N_{(Al+BO)}$ the fraction of the bridging oxygen (BO) in the Al tetrahedral unit, i is the component of melt except SiO_2, i.e. CaO, MgO FeO, K_2O, Na_2O, Al_2O_3, and j is the charge-compensating ion from component i except Al_2O_3, i.e. Ca^{2+}, Mg^{2+}, Fe^{2+}, K^+ and Na^+.

Table 2. Component parameters in the viscosity model.

M_xO_y	α_i	j	$\alpha_{j\,in\,Al}$
CaO	4	Ca2+	1.46
MgO	3.43	Mg2+	1.56
FeO	6.05	Fe2+	3.15
K2O	6.25	K+	-0.69
Na2O	7.35	Na+	0.27
CrO	3	Cr2+	0.6
Cr2O3	4.7	Cr3+	5
NiO	6.05	Ni2+	3.15
TiO2	4	Ti4+	1.46
Fe2O3	6.05	Fe3+	3.15
UO2	0.5	U4+	3
ZrO2	0.65	Zr4+	5
Al2O3	1.14		

Slag system is divided into three groups of species, a) SiO_2, b) M_xO_y (CaO, MgO, FeO, K_2O, Na_2O, ...) and c) Al_2O_3. Then relative mole numbers for these groups are calculated so that:

$$a + \sum_i b_i + c = 1 \tag{5}$$

Sum of fractions $N_{(NBO+FO)i}$ and $N_{(Al+BO)j}$ are calculated as:

$$N_{(Al-BO)_j} = \frac{n_{(O-Al\,in\,Al)_j}}{n_{Total-O}} = 4c\left(b_i \Big/ \sum_i b_i\right) \Big/ \left(2a + \sum_i b_i + 3c\right) \qquad \sum_i b_i \geq c$$

$$N_{(Al-BO)_j} = \frac{n_{(O-Al\,in\,Al)_j}}{n_{Total-O}} = 4b_i \Big/ \left(2a + \sum_i b_i + 3c\right) \qquad \sum_i b_i < c \tag{6}$$

$$N_{(NBO-BO)_i} = \frac{n_{(O-M)_i}}{n_{Total-O}} = \left\{b_i - c\left(b_i \Big/ \sum_i b_i\right)\right\} \Big/ \left(2a + \sum_i b_i + 3c\right) \quad \sum_i b_i \geq c$$

$$N_{(NBO-BO)_i} = \frac{n_{(O-M)_i}}{n_{Total-O}} = 3\left(c - \sum_i b_i\right) \Big/ \left(2a + \sum_i b_i + 3c\right) \qquad \sum_i b_i < c \tag{7}$$

The volume fraction of precipitated solids affects the effective viscosity of the slag. Mostafaee [4] gives following correlation for the effective viscosity:

$$\mu = \mu_0\left(1 + 5.5V_f\right) \tag{8}$$

where μ_0 is the viscosity of the slag phase and V_f is the volume fraction of solids in the system.

Viscosity model does not require SiO_2 or Al_2O_3 to be present. For example if they both are zero then $N_{(NBO+FO)i}$ is simplified to mole fraction of B_i.

Viscosity model (without UO_2 and ZrO_2) has been validated with chromium [5] and non-chromium [6] containing slags for steel making. Figure 7 shows the correlation between measure and calculated viscosities.
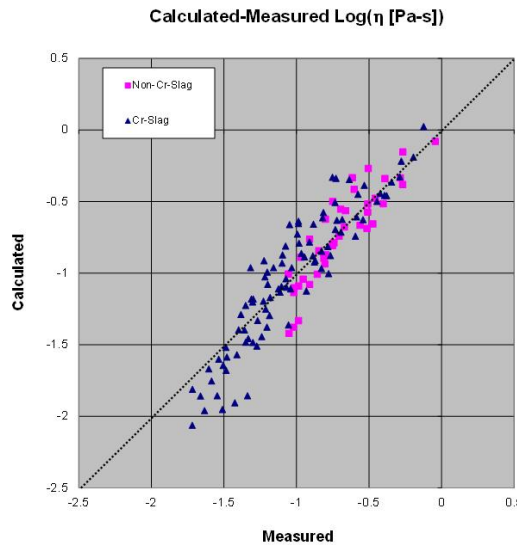

Figure 7. Correlation between measured and calculated viscosity data [5, 6].

2.8 Density model

Density of the slag is calculated from its molar volume V_m and molar weight M:

$$\rho = \frac{M}{V_m} \tag{9}$$

$$V_m = \sum_i x_i \overline{V}_i \tag{10}$$

where x_i is the mole fraction and $\overline{V}_i$ partial molar volume of compound i. Here the partial molar volumes are assumed to be equivalent to the molar volumes of pure compounds.

Table 3 shows the molar volumes of the included pure compounds.

Table 3. Molar volumes of pure compounds [7, 8].

Compound	Molar volume of pure compounds (cm³/mol)	V_m @ 1600 °C	V_m @ 1700 °C
Al_2O_3	28.3 * (1 + 0.0001 * (T - 1773))	28.583	28.866
B_2O_3	45.8 * (1 + 0.0001 * (T - 723))	51.068	51.526
CaF_2	31.3 * (1 + 0.0001 * (T - 1773))	31.613	31.926
CaO	20.7 * (1 + 0.0001 * (T - 1773))	20.907	21.114
CrO	30.1 * (1 + 0.0001 * (T - 1773))	30.401	30.702
Cr_2O_3	30.1 * (1 + 0.0001 * (T - 1773))	30.401	30.702
FeO	15.8 * (1 + 0.0001 * (T - 1773))	15.958	16.116
Fe_2O_3	15.8 * (1 + 0.0001 * (T - 1773))	15.958	16.116
K_2SO_4	93.7	0.000	0.000
MgO	16.1 * (1 + 0.0001 * (T - 1773))	16.261	16.422
MnO	15.6 * (1 + 0.0001 * (T - 1773))	15.756	15.912
Na_2O	33 * (1 + 0.0001 * (T - 1773))	33.330	33.660
Na_2SO_4	72.1	0.000	0.000
NiO	30.1 * (1 + 0.0001 * (T - 1773))	30.401	30.702
SiO_2	27.516 * (1 + 0.0001 * (T - 1773))	27.792	28.067
TiO_2	18.8 * (1 + 0.0001 * (T - 2143))	18.293	18.481

2.9 Surface tension model

The surface tension of silicate melts plays important roles in the processes at high temperature. Tanaka et al. applied thermodynamic databases to evaluate the surface tensions of liquid alloys, ionic melts and oxide melts by using a model based on Butler's equation. Recently, Tanaka et al. [7] have developed a new model for evaluating the surface tension of molten silicates, which takes into consideration the ionic radii of the components. This particular model can be readily applied to many kinds of molten ionic mixtures and molten slags, because the surface tension of silicate melts can be calculated using the information on the surface tensions and molar volumes of pure oxides, as well as the cationic and anionic radii of the component oxides in the system.

Butler equation to calculate the surface tension of compound in ionic mixture is given as:

$$\sigma_i = \sigma_i^{pure} + \frac{RT}{A_i} \ln \frac{M_i^s}{M_i^b} \tag{11}$$

where R is the gas constant, T is the temperature and A_i is the molar area of the compound i:

$$A_i = N_0^{1/3} V_i^{2/3} \tag{12}$$

where N_0 is Avogadro number and V_i the molar volume of compound i. M_i term is given as:

$$M_i^\alpha = \frac{\dfrac{R_i^C}{R_i^A} x_i^\alpha}{\sum_i \dfrac{R_i^C}{R_i^A} x_i^\alpha} = x_i^\alpha \gamma_i^\alpha \qquad \left(\gamma_i^\alpha = \frac{\dfrac{R_i^C}{R_i^A}}{\sum_i \dfrac{R_i^C}{R_i^A} x_i^\alpha} \right) \tag{13}$$

where α is either the bulk (b) or the surface (s) phase, x the mole fraction of compound i in phase α, R is the radius of ion and C denotes the cation and A the anion of compound i.

Surface tension of pure compounds σ^{pure} are given in Table 4.

Table 4. Surface tensions of pure slag compounds [7, 8].

Compound	Surface tension of pure compound (mN/m)	σ @ 1600 °C	σ @ 1700 °C
Al_2O_3	1024 - 0.177 * T	692.452	674.752
B_2O_3	37.9 + 0.0354 * T	104.210	107.750
CaF_2	1604.6 - 0.72 * T	255.932	183.932
CaO	791 - 0.0935 * T	615.860	606.510
CrO	185.5 + 0.0984 * T	369.818	379.658
Cr_2O_3	625.5 + 0.0984 * T	809.818	819.658
FeO	504 + 0.0984 * T	688.318	698.158
Fe_2O_3	25.5 + 0.0984 * T	209.818	219.658
K_2SO_4	140.6	140.600	140.600
MgO	1770 - 0.636 * T	578.677	515.077
MnO	988 - 0.179 * T	652.706	634.806
Na_2O	438 - 0.116 * T	220.715	209.115
Na_2SO_4	185	185.000	185.000
NiO	470.5 + 0.0984 * T	654.818	664.658
SiO_2	243.2 + 0.031 * T	301.268	304.368
TiO_2	573 + 0.09 * T	741.584	750.584

2.10 Iterative method for solving the surface tension

Surface tension can be solved by using fixed point iteration scheme.

1. Initial surface tension and molar fractions at surface are guessed:

$$\sigma_1^s = \sigma^0 \tag{14}$$

$$x_1^s = x_i^b \tag{15}$$

2. Activity coefficients of species are calculated using equation (13).

3. Mole fractions of species at surface are solved from equation (16) and scaled to one (initially the sum of mole fractions could be a relatively large number (>>1).

$$x_i^s = \exp\left(\frac{(\sigma^s - \sigma_i^s)A_i}{RT} + \ln x_i^b \gamma_i^b - \ln \gamma_i^s\right) \tag{16}$$

$$x_i^s = \frac{x_i^s}{\sum x_i^s} \tag{17}$$

4. New estimate for surface tension is calculated using equation (11) (for example the weighted average of all compounds).

5. Steps 2, 3 and 4 are repeated until surface tension and mole fractions at surface converge.

Convergence can be made faster by using a speeding method like Steffensen's three point extrapolation method, but usually only a few iterations are required for the convergence. Also systems with very non-linear activities converge quite easily.

2.11 Magnetism model

Oulu University conducted experiments using external magnetic field to affect the chemical equilibrium of molten slag although these experiments proved to be very challenging at high temperatures. This raised interest to further investigate if **CFE**-method developed by Pajarre and Koukkari [9] could be applied to external magnetic field.

In physics, the susceptibility of a material or substance describes its response to an applied field, either electric or magnetic. In electromagnetism, the magnetic susceptibility χ (Latin: susceptibilis "receptiveness") is a dimensionless proportionality constant that indicates the degree of magnetization of a material in response to an applied magnetic field.

$$M = \aleph H \tag{18}$$

where M is the magnetization of the material (the magnetic dipole moment per unit volume), measured in amperes per meter and H is the magnetic field strength, also measured in amperes per meter. The magnetic susceptibility of most crystals is not a scalar. Magnetic response M is dependent upon the orientation of the sample.

If χ is positive, the material can be paramagnetic. In this case, the magnetic field in the material is strengthened by the induced magnetization. Alternatively, if χ is negative, the material is diamagnetic and the magnetic field in the material is weakened by the induced magnetization. Generally, non-magnetic materials are said para- or diamagnetic because they do not possess permanent magnetization without external magnetic field. Ferromagnetic, ferrimagnetic, or

antiferromagnetic materials, which have positive susceptibility, possess permanent magnetization even without external magnetic field.

2.12 Magnetism and chemical potential

An applied magnetic field has a direct thermodynamic influence on the chemical potential (Gibbs free energy) of the various phases in a material. This is clearly shown in the following equation for calculating the Gibbs free energy change for iron for the ferrite, α, to austenite, γ, phase transformation in a Fe-C binary alloy in the presence of an applied magnetic field:

$$\Delta G^{\gamma \to \alpha} = RT\left(\ln a_{Fe}^{\gamma} - \ln a_{Fe}^{\alpha}\right) + \int_{0}^{H}\left(M_{Fe}^{\gamma} - M_{Fe}^{\alpha}\right)dH \qquad (19)$$

2.13 Example: Hypereutectoid Steel Investigation

Ludtka's research report [10] shows experiments performed with the 1045 steel to investigate the influence of different continuous cooling rates on austenite decomposition transformation behaviour while a constant 30-T magnetic field was applied. For accelerated cooling, a helium gas quench can be rapidly imposed upon the specimen. Such a system allows for the entire thermal cycle or any portion of it to be exposed to a high magnetic field. A 32-mm-diam-bore magnet with a maximum field strength of 33 T was used for the experiments. A key component of the experimental work was the ability to heat and cool the specimen while inside the bore of the magnet. A custom-designed induction heating coil, coupled with a gas purge system for atmosphere control and specimen cooling, was fabricated for the experiments. The apparatus can heat the steel specimen, located in the centre of the bore mid-length, up to 1100ºC and maintain the high temperature for extended periods of time.
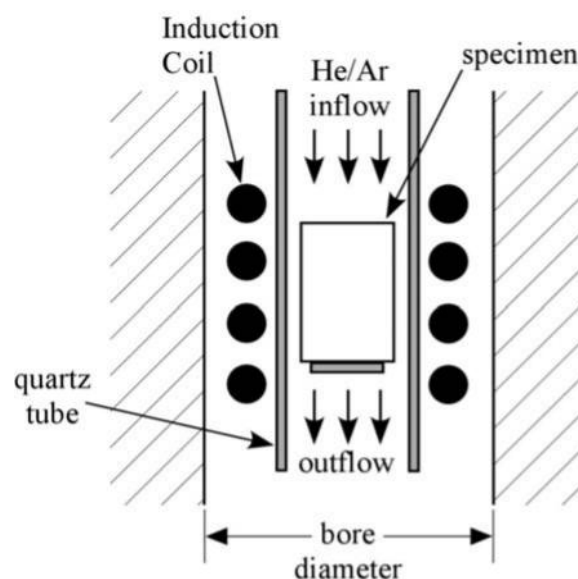

Figure 8. Experimental device [10].

Series of experiments run on the 1045 steel were conducted to determine the shift in the austenite decomposition transformation temperature as a function of magnetic field strength and to obtain an estimate of the Gibbs free energy contribution due to the magnitude of an applied magnetic field.

Table 5. Composition of the 1045 steel [10].

C	0.45w-%
Si	0.15w-%
Mn	0.80w-%
P	0.04w-%
S	0.05w-%
Fe	Balance

These were determined by conducting identical cooling rate experiments at magnetic field strengths of 0, 10, 20, and 30 T. The alloy undergoes a paramagnetic to ferromagnetic transformation during cooling that approximately correlates with the austenite phase decomposition process (Figure 9), applied during the entire cooling cycle from the austenitization temperature. To obtain the shift in transformation temperature between the no-field vs. applied-field conditions, the derivatives of the cooling curve data with respect to time, dT/dt, were obtained and plotted vs temperature to determine the point at which the greatest rate of change was observed. This maximum dT/dt point was defined as the transformation initiation temperature for that condition. The shifts in transformation temperature between the no-field and the magnetic field strength conditions are also summarized in the middle column of Table 6. These data are plotted vs. magnetic field strength in Figure 10. The shift in transformation temperature per tesla of applied field for this alloy is quantified by a slope of ~3°C/T. The alloy undergoes a paramagnetic to ferromagnetic transformation during cooling that approximately correlates with the austenite phase decomposition process.
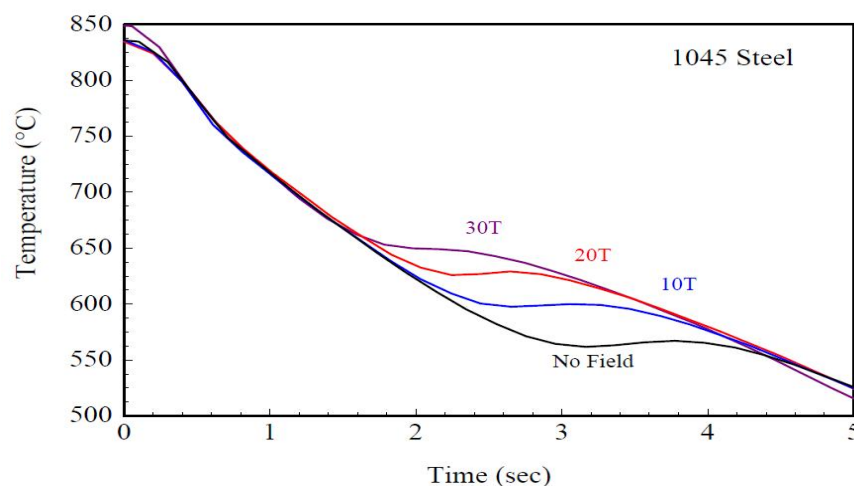

Figure 9. Continuous cooling path information for the 1045 low carbon steel alloy for different magnetic field strengths [10].
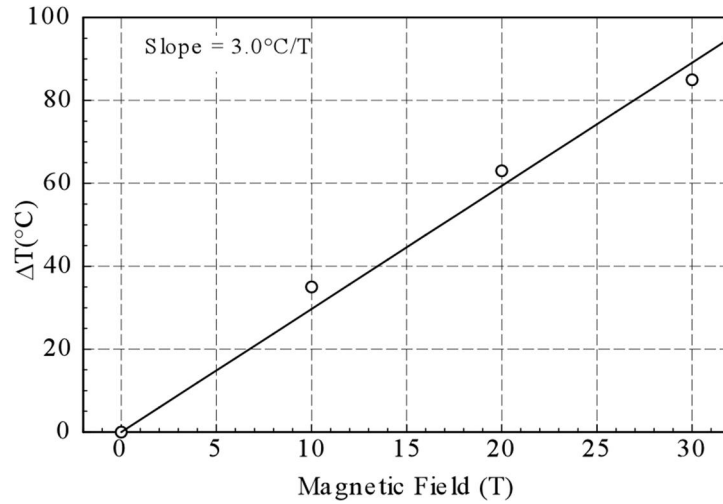
Figure 10. Plot of the experimental transformation temperature shifts [10].

Table 6. Experimentally derived magnetic field contribution to Gibbs energy [10].

B (tesla)	$\Delta T = T^B - T^0$, (C)	$\Delta G^{B, \gamma \to \alpha}$ (J/mol)
10	35	150
20	63	265
30	85	360

Estimate of the Gibbs free energy change for the austenite decomposition transformation due to the presence of the magnetic field can be given as [10]:

$$G^{\gamma \to \alpha} + G^B = \left(\frac{H^{\gamma \to \alpha}}{T^{Eq}} \right)\left(T^{Eq} - T^B \right) \qquad T^{Eq} = 720^0 C, H^{\gamma \to \alpha} = 4200\,J/mol \quad (20)$$

where T^B is the transformation temperature under the application of the magnetic field of strength B. Plotting magnetic free energy contributions, G^B, vs magnetic field strength gives a slope of 12.6 J/mol ·T, as shown in Figure 11.
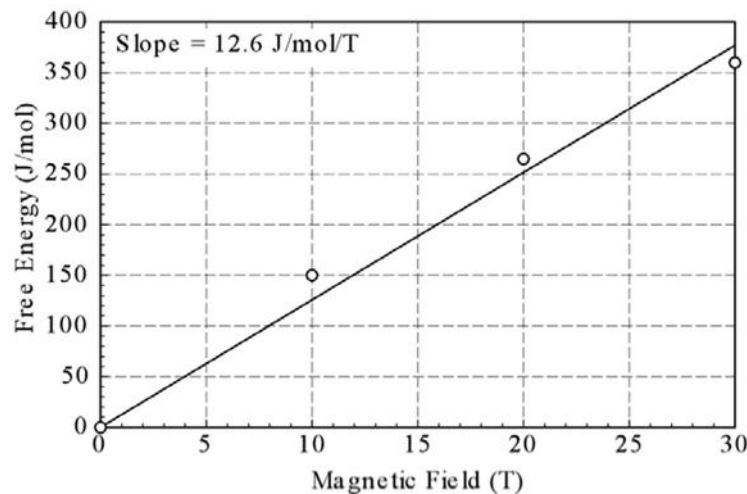

Figure 11. Plot of the experimentally estimated magnetic contribution to the Gibbs free energy as a function of magnetic field strength [10].

Figure 12 shows the pseudobinary phase diagram predicted by **ThermoCalc**-software for both a conventional equilibrium condition and the magnetically enhanced circumstance.
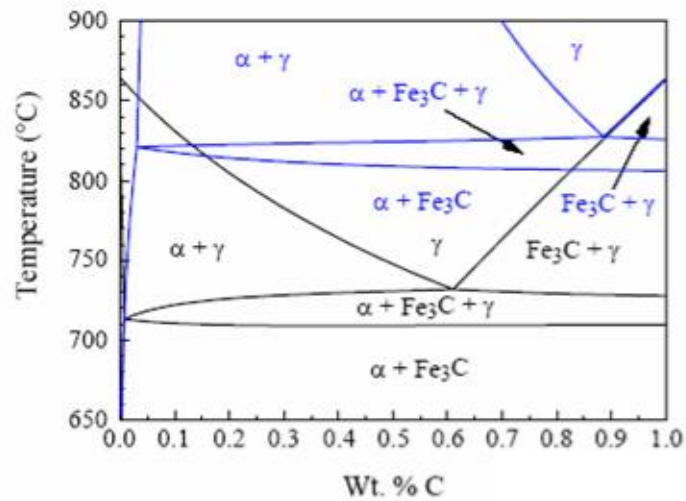

*Figure 12. Prediction of the pseudobinary phase diagram for 1045 steel for conventional equilibrium (black lines) and magnetically enhanced equilibrium (blue lines). Calculated with **ThermoCalc** [10].*

Clearly evident in the predicted phase diagrams is that magnetic fields:

1. raise phase transformation temperatures,
2. increase the solubility of carbon in the various phases, and
3. shift critical congruent points such as eutectoid chemistries and temperatures.

According to Ludtka [10] his study definitively demonstrates that the materials scientist is no longer limited to just one phase diagram per alloy chemistry when considering alloy development, heat treatment, and thermomechanical processing approaches to optimize microstructure and phase transformation kinetics and to enhance material properties. Magnetic processing now enables a continuum (3D with the added dimension of magnetic field strength, H) of phase diagrams to be developed for any alloy. the added dimension of magnetic field strength, H) of phase diagrams to be developed for any alloy. Since the thermodynamic dependence of the Gibbs free energy is linear with H, the only limit to this technology will be the magnetic field strengths available in commercial magnets, which are improving all the time. An implication of these predictions is that magnetic field processing can be used to isothermally transform a material.

2.14   Magnetism and CFE-Method

Chemical potential of any species in thermodynamic system is given as linear combination chemical potentials of independent variables of the system (system components), for binary system where system components are x and y:

$$\mu(x_a y_b) = a\pi_x + b\pi_y \qquad (21)$$

where a and b are stoichiometric coefficients of system components x and y in species and p is the chemical potential of a system component or also known as Lagrangian multiplier of the system.

Magnetism can be added as a new constrain by introducing a new pseudo system component M:

$$\mu^*(x_a y_b) = \mu(x_a y_b) - M \cdot H = a\pi_x + b\pi_y + v_M \pi_M \quad v_M = -\frac{M}{M_0}, \; M_0 = \frac{J}{molK} \; (22)$$

Table 7 shows an example of stoichiometry with elements Fe, C and additional magnetic field strength M* system component:

Table 7. Stoichiometric system with additional magnetic field strength M*.

Phase	Species	System component		
		Fe	C	M*
BCC-FER	Fe:C	1	3	-12.6
	Fe:Va	1	0	0
FCC-AUS	Fe:C	1	1	0
	Fe:Va	1	0	0
FeC3	Fe3C	3	1	0
M	M	0	0	1

There is also additional M phase (pure condensed phase) that normally has chemical potential zero (no magnetic field situation). Its pseudo chemical potential can be set to positive value (for example in ChemSheet calculation) that corresponds wanted magnetic field strength. Then this will directly affect the chemical potential of the ferritic iron (BCC/Fe:C). For example with magnetic field strength 20 T chemical potential of Fe:C is changed by 252 J/mol (12.6*20.0). Value 12.6 [J/mol·T] is taken from the slope in Figure 11.

3 Results

3.1 Observed foaming at Tornio

CSFoam tool was used to calculate the observed foaming at Tornio steel-factory. Table 8 shows the observed foaming and the respective measured compositions of the slag phase.

Table 8. Example of observed foaming at Tornio steel-factory. The fifth column contains the observed foaming and the columns 5-17 the measured slag composition.

PPAIKKA	SULNRO	LAATU	LAATURY	KUOHUMINEN	Cr2O3	Fe2O3	Al2O3	MgO	CaO	SiO2	MnO	TiO2	V2O5	Ni	S	P	CaO/SiO2	E-aste	SP-kerr
													NÄYTE 707						
VKU 2	11944	720-1	RU	2	2.7	1.2	10.9	6.5	43.2	24.7	1.5	3.1	0.08	0.05	0.15	0.012	2.01	1.29	11.72
VKU 2	11942	720-1	RU	1	2.9	1.2	12.1	6.3	45.9	21.2	1.2	3.3	0.09	0.05	0.22	0.013	2.46	1.42	12.81
VKU 2	11938	720-1	RU	1	2.1	1.2	11.8	5.4	47.9	23.8	1	2.4	0.06	0.06	0.23	0.012	2.24	1.41	12.68
VKU 2	11936	720-1	RU	1	2.1	1.2	12.1	5.2	47.1	23.5	1.1	2.8	0.07	0.05	0.22	0.012	2.23	1.36	12.91
VKU 2	11934	720-1	RU	1	3.6	1.3	12.3	5.2	45.8	22.3	1.6	2.9	0.12	0.06	0.29	0.012	2.29	1.36	12.43

Observed foaming value 1 equals to no foaming, 2 to slight foaming, 3 heavy foaming and 4 excess foaming (overflow).

ChemSheet with a thermodynamic system extracted from FSstel and FToxid database was used to calculate the equilibrium of the slag phase. This yielded the mass fractions of solid phases at equilibrium as well as the equilibrium composition of the remaining slag phase. Then CSFoam-tool was used to calculate the foaming index of the slag so that the mass fraction of solids were taken into consideration in the calculation of the viscosity by using the equation (8). The calculated foaming values were scaled between 0.5 and 4.5.
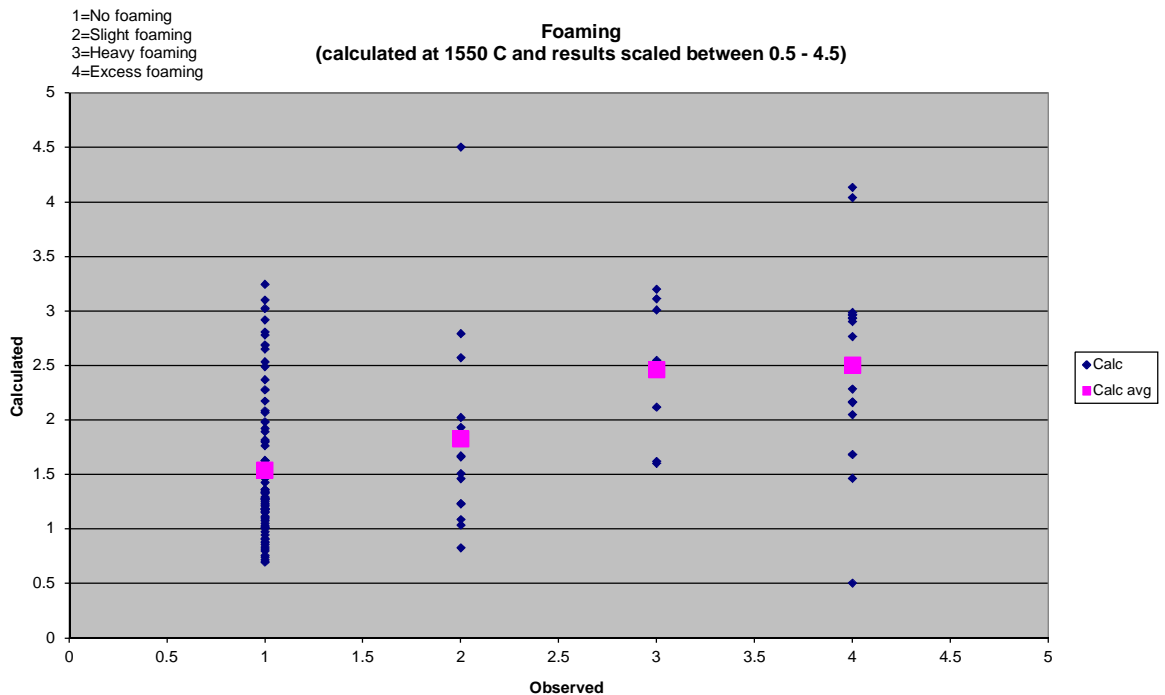

Figure 13. Relative foaming indices. The x-axis contains the observed and the y-axis the calculated values. The calculated values are scaled between 0.5 and 4.5 where 1 equals to no foaming, 2 to slight foaming, 3 heavy foaming and 4 excess foaming (overflow).

3.2 EAF Model Results For VKU2 Furnace

Table 9 shows the composition of the raw materials in VKU2 furnace.

Table 9. Example composition of raw materials in VKU2 furnace.

Baskets	Mass/kg
Al	534.582
C	1618
Cr	28007.5
Fe	94456.47
Mn	1871.723
Ni	10281.5
Si	1569.057
Ti	351.608
Sum	138690.4

Lime	Mass/kg
CaO	4760
MgO	790.8

Air	Mass/kg
N2	18582
O2	6083

Carbon	Mass/kg
C	300

Figure 14 shows the composition of the slag phase as function of temperature.
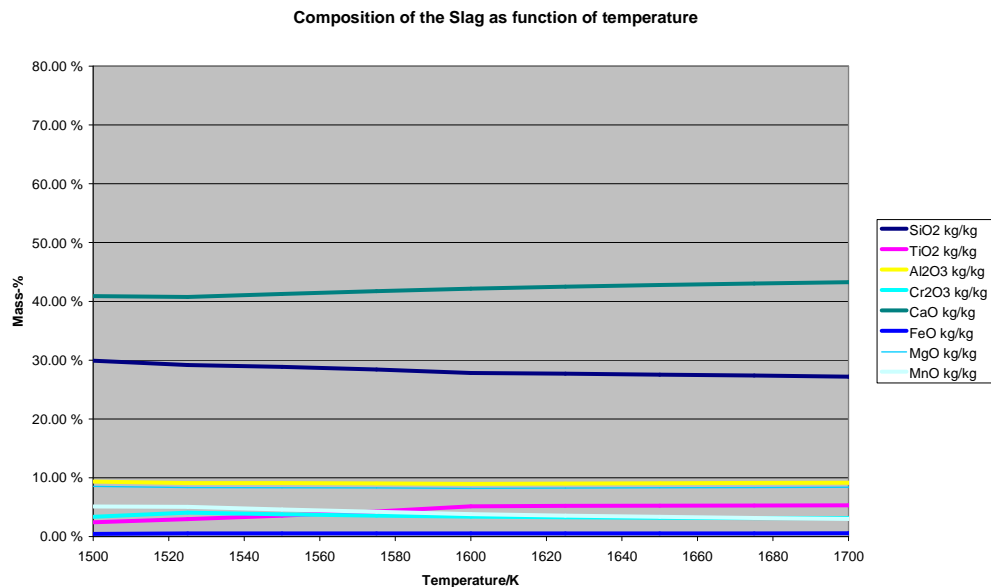

Figure 14. Slag composition as function of temperature.

Figure 15 shows the calculated slag phase composition and Figure 16 shows the calculated steel phase composition at 1600 degrees Celsius. The calculated slag mass fraction and basicity were 7.7% and 1.5, respectively.
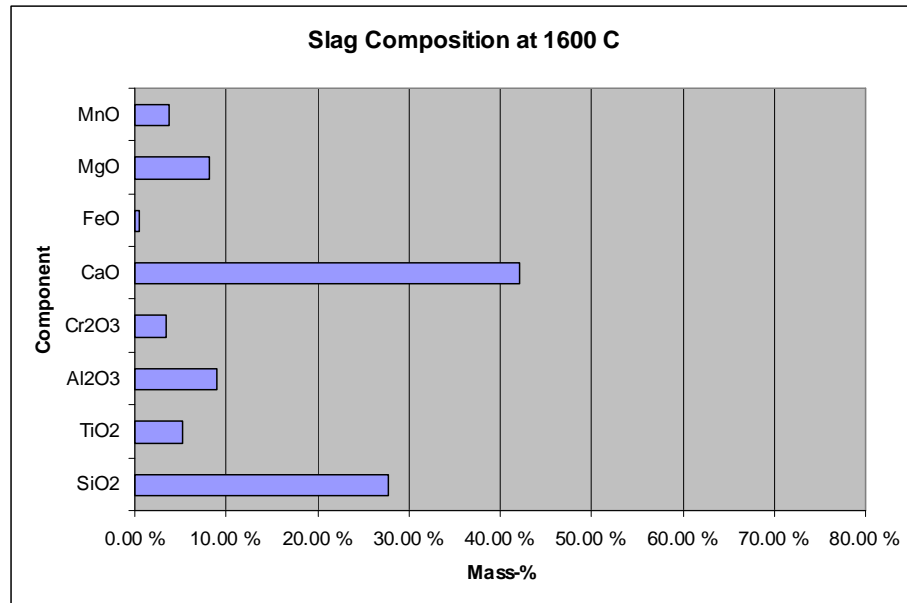
Figure 15. *Slag composition at 1600 degrees Celsius. Slag mas fraction 7.7%, slag basicity 1.5.*
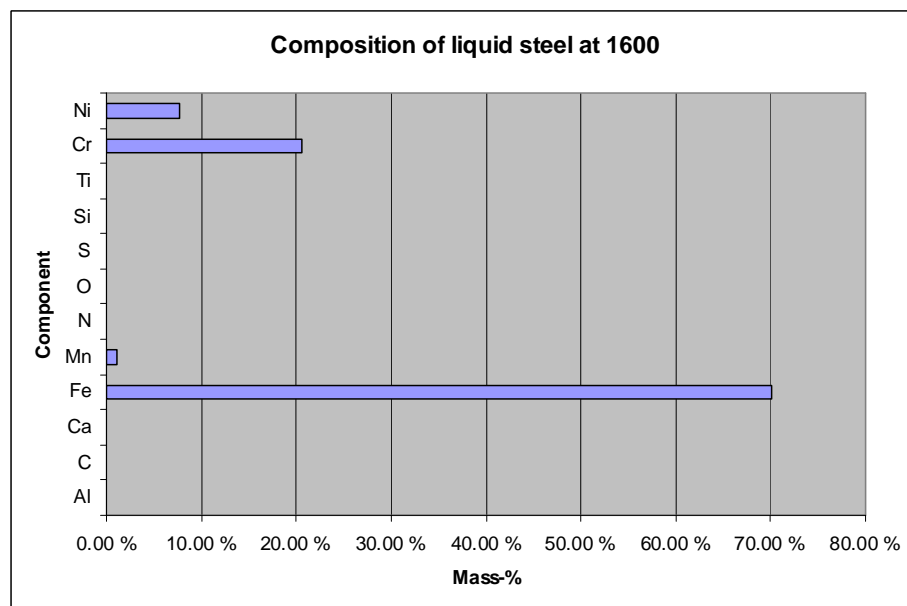
Figure 16. *Liquid composition at 1600 degrees Celsius.*

Figure 17 shows the calculated foam index at 1600 degrees Celsius as function slag basicity. It can be seen that both the viscosity and foam index are strongly dependent on the slag basicity.
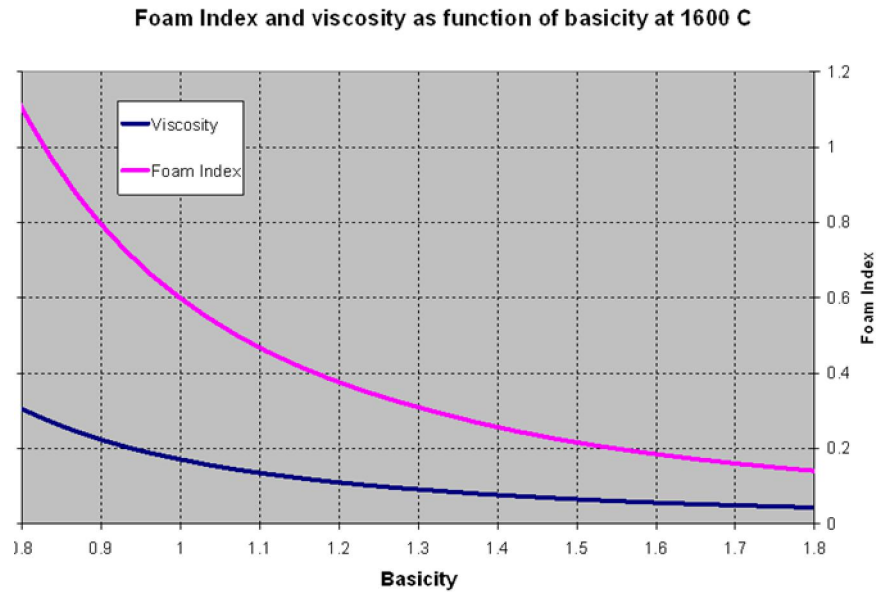
Figure 17. Foam index and viscosity as function of basicity at 1600 °C.

3.3 Magnetic Field Strength Results

ChemSheet model was made for Fe-C system with additional magnetic field strength constrain as described in Chapter 2.14. Figure 18 shows the calculated phase diagram as function of magnetic field strength.
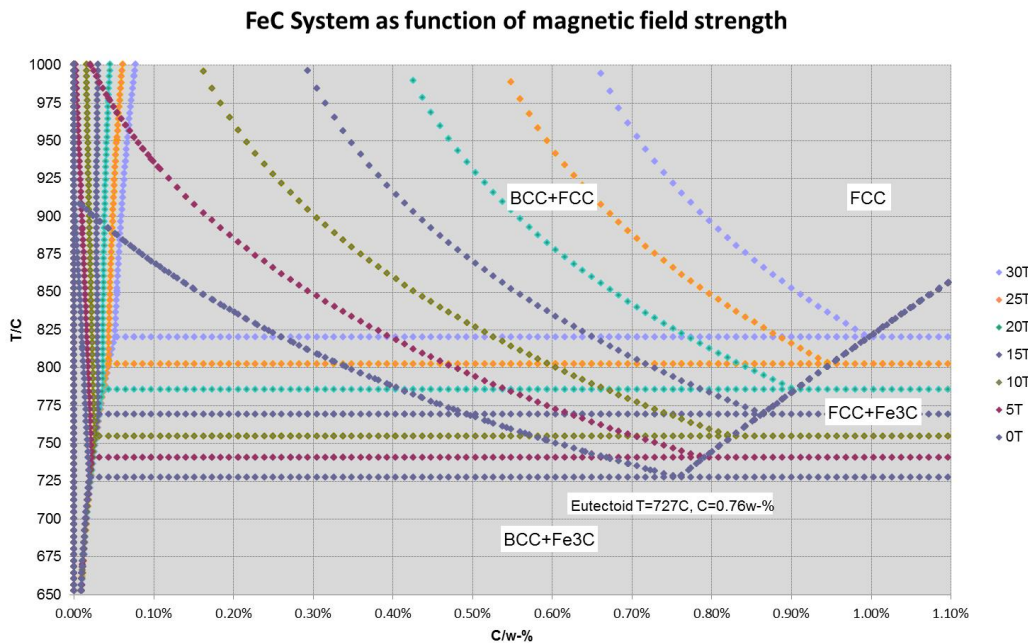

Figure 18. Phase diagram for Fe-C system as function of magnetic field strength.

4   Conclusions

Thermodynamic database **FactSage** was used to compile a thermodynamic system for the electric arc furnace. Thermodynamic system was compiled from **FToxid** and **FSstel** databases. They are intended to provide a sound basis for calculations covering a wide range of steelmaking processes.

ChemSheet model was made to calculate the chemical composition of the slag-steel-solid inclusions -system in the furnace as function of temperature.

CSFoam-tool was developed to calculate the foaming index of the slag phase. The foaming index depends on the physical properties of the slag phase, i.e. its density, surface tension and viscosity. The viscosity of the slag phase is very dependent on its SiO_2-content. Higher SiO_2-content increases the viscosity. **CSFoam**-tool was used to calculate the observed foaming at Tornio steel-factory with measured temperatures and furnace compositions**.** The calculated relative foaming index values show some resemblances to the measured values.

ChemSheet model was made for Fe-C system with additional magnetic field strength constrain to calculate the phase diagram of Fe-C system. Calculated values show that increasing the magnetic field strength increases the eutectoid point of the system (by 100 °C at 30 T). Clearly evident in the predicted phase diagrams is that magnetic fields:

1. raise phase transformation temperatures,
2. increase the solubility of carbon in the various phases, and
3. shift critical congruent points such as eutectoid chemistries and temperatures.

5   Summary

A good slag practice is essential for production of a high-quality stainless steel. In addition, the electrical and material efficiency of the electric arc furnace can considerably be improved by a good slag practice. The metallurgical properties of the slag are strongly influenced by its high-temperature microstructure. Thus, characterization of the phases within the **EAF** slag as well as the determination of the amount of these phases and their compositions is of high importance.

This report described development and validation of advanced computational methods for thermophysical properties of the steel-inclusion system, like density, surface tension and viscosity of the slag phase. Also the effect of magnetic field strength on solidification of steel was studied. A phase diagram of a simple Fe-C system as function of magnetic field strength was calculated by using a special **ChemSheet** model. **CSFoam**-tool was developed to calculate the foaming index of the slag by using the aforementioned thermophysical properties. The foaming index is a parameter that quantifies the ability of slag to generate foam from either injected gas or gas that is generated within the slag or metal.

References

1. Liukkonen, M.; Penttilä, K.; Koukkari, P., "A compilation of slag foaming phenomenon research. Theoretical studies, industrial experiments and modelling," VTT, 2012, 128p. VTT Technology 63, ISBN 978-951-38-7897-9 (URL: http://www.vtt.fi/publications/index.jsp).

2. Hack, K., Petersen, S., Koukkari, P. and Penttilä, K., "CHEMSHEET an Efficient Worksheet Tool for Thermodynamic Process Simulation", Microstructures, Mechanical Properties and Processes, Bréchet Y., Wiley (Ed.), EUROMAT, Vol. 3, 1999, pp. 323-330.

3. Nakamoto, M., Miyabashi, Y., Holappa, L., and Tanaka, T., "A Model for Estimating Viscosities of Aluminosilicate Melts Containing Alkali Oxides", ISIJ International, Vol. 47, No. 10, 2007, pp. 1409–1415.

4. Mostafaee, S., A Study of EAF High-Chromium Stainless Steelmaking Slags Characteristics and Foamability, Doctoral Thesis, Department of Materials Science and Engineering, Division of Applied Process Metallurgy, Stockholm, 2011, 78 p.

5. Forsbacka, L., Holappa, L. "Viscosity of SiO_2-CaO-CrO_x slags in contact with metallic chromium and application of Iida model", VII International Conference on Molten Slags Fluxes and Salts, The South African Institute of Mining and Metallurgy, 2004.

6. Measured viscosity data from Nakamoto, M., Osaka University.

7. "Nakamoto, N., Tanako, T., Holappa, L., Hämäläinen M., Surface Tension Evaluation of Molten Silicates Containing Surface-active Components (B_2O_3, CaF_2 or Na_2O)", ISIJ International, Vol. 47, 2007, 211–216.

8. Hanao, M., Tanaka, T., Kawamoto, M., Takatani, K., "Evaluation of Surface Tension of Molten Slag in Multi-component Systems", ISIJ International, 47, 2007, 935-939.

9. Koukkari, P., Pajarre, R., "A Gibbs energy minimization method for constrained and partial equilibria", Pure Appl. Chem. , 83, 2011, 1243-1254.

10. Ludtka, G., M., "Exploring Ultrahigh Magnetic Field Processing of Materials for Developing Customized Microstructures and Enhanced Performance", Oak Ridge National Laboratory, 2005, Technical Report, ORNL/TM-2005/79.